Effect of trans-cinnamaldehyde or citral on sodium caseinate: Interfacial rheology and fluorescence quenching properties

Wei Liao, Abdelhamid Elaïssari, Emilie Dumas, Adem Gharsallaoui

Effect of trans-cinnamaldehyde or citral on sodium caseinate: Interfacial rheology and fluorescence quenching properties

Graphical abstract:

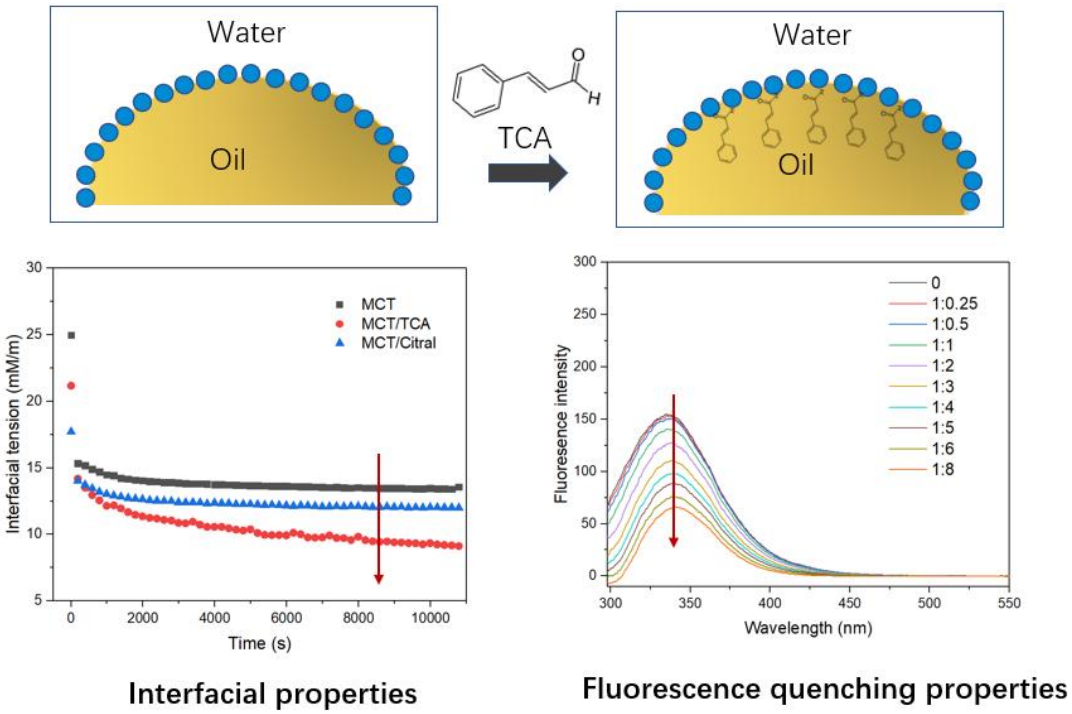

Highlights:

- TCA and citral addition results in lower interfacial tension at O/W interface for CAS solution.
- TCA addition enhances the surface dilatational module of O/W interfacial film.
- The binding between TCA and CAS involves hydrogen bonding with confirmation change.
- The binding between TCA and caseinate is spontaneous.

Abstract:

Trans-Cinnamaldehyde (TCA) and citral are the major components of cinnamon oil and lemongrass oil, respectively, which have a variety of functional properties. The interaction between CAS and these two aldehydes was studied by interfacial properties and fluorescence quenching measurements. The data of protein adsorption in the O/W interface indicated that mixing a small amount of TCA or Citral into the oil phase can both decrease the interfacial tension and the effect of TCA was more prominent. Meanwhile, the use of TCA improved the diffusion rate (K_{diff}) in the initial absorption stage and developed a stronger interface with higher moduli. The fluorescence quenching test showed that TCA has a more obvious quenching effect on CAS than citral. Further kinetic analysis of the binding between CAS and TCA indicated that both dynamic and static quenching occurs. The large binding constant (1.78×10^5 M^{-1}) at 25 ° C was calculated by Stern-Volmer equation which suggests that TCA has strong affinity for CAS. Moreover, this bonding process is spontaneous, as suggested by negative free energy change. The negative enthalpy and negative entropy change also suggested that the binding is driven by formation of hydrogen with unfavorable conformational change. This work would provide some guidance for by using the binding properties with some nature aldehydes to enhance the interface properties of protein.

Keywords: Sodium caseinate (CAS); *trans*-Cinnamaldehyde (TCA); Citral; Interfacial properties; Fluorescence quenching;

Introduction:

Many food products are based on emulsions systems (O/W and W/O) (X. Zhang et al., 2021) which require the use of emulsifying agents to stabilize the interface between different phases. Nowadays, food industries prefer to use more nature emulsifiers like proteins rather than chemical synthetic emulsifiers (Felix et al., 2019), since these proteins can providing extra nutritional added values and are more acceptable by consumers. Some proteins such as soy, pea, gelatin, dairy protein have been reported as emulsifiers with good surface activity at the interface, which can adjust the interfacial properties of emulsion systems by partially spreading their hydrophobic groups to the oily phase (Fuller and Vermant, 2012; Ribeiro et al., 2021). During the absorption process, protein molecular general unfold and expose numbers of hydrophobic residues which may physically or chemically interact with other functional compounds, thereby altering their functional performance (Dickinson, 1989). Different active compounds introduced to protein based systems to tailor their solubility, hydrophobicity, dispersibility and surface charge by using of some enzyme or crosslinking agents (Fischer and Windhab, 2011; Glusac and Fishman, 2021; Tann et al., 2001). However, these treatments may introduce a new function group of components which is generally limited in the food section due to toxicity and absence of GRAS status. Therefore, more natural compounds for protein functionalization should be search and investigated.

Among flavor compounds, aldehydes have an vital role in flavor development of food products (Wang et al., 2021). It was reported that certain aldehydes are able to interact with various functional residues of amino groups, like ε-amino groups of lysine, the sulfhydryl group of cysteines, the imidazole ring of histidines and the phenol group of tyrosines, etc (Azeredo and Waldron, 2016; Habeeb and Hiramoto, 1968). Specific cases include the some aromatic aldehydes such cinnamaldehyde, salicylaldehyde, syringaldehyde, vanillin and anisaldehyde, have been introduced in food and pharmaceutical industries (Banerjee and Chattopadhyay, 2019; Boeve and Joye, 2020). These aromatic aldehydes have gained considerable attention since their various health benefits like anti-inflammatory, antioxidant, antimicrobial agents and anticancer properties (Banerjee and Chattopadhyay, 2019). *Trans*-cinnamaldehyde (3-phenyl-2-propenal, TCA, FEMA 2286) is a major component of volatile cinnamon essential oil (Adams et al., 2004). It showed broad-spectrum antimicrobial activity against bacteria, yeast, and molds (Shen et al., 2015). Citral

(3,7-dimethyl-2, 6-octadienal, FEMA 2303) is main component of citrus fruit's peel oil which is widely applied as a flavoring additive in foods and beverages (Zhang et al., 2020). As these two active compounds are extremely low solubility in water, it is difficult to prepare food formulations containing these nature aldehydes in solubilized form. There are two main approaches to overcome the insolubility issues: 1) mixing them with carrier oils and then producing it in the form of oil-water systems by some food component emulsifiers since these aldehydes show well solubility in oil; 2) introducing them with a food component may provide a way to deliver nature aldehydes since several reports showed that some aldehydes are properly able to bond with proteins (Asghari et al., 2017; Felix et al., 2019; Weibel and Hansen, 1989). A combination of van der Waals forces, electrostatic forces, hydrogen binding and/or hydrophobic binding may contribute to protein-aldehydes interactions and this should be further analyzed. Several studies reported that aldehydes can bind with amino acid residues of proteins by irreversible covalent binding (Guo et al., 2020), hydrophobic interaction (Wang and Arntfield, 2015) or hydrogen bonding (Tan and Siebert, 2008; Weel et al., 2003), which depend on the specific chemistry and structure of the interacting molecules. Meanwhile, the binding between aldehydes and proteins could be also used in oil in water interface to adjust the interfacial properties. However, the relative reports about the mechanisms of interaction between aromatic aldehydes and protein are still scarce.

Sodium caseinate (CAS) is heterogeneous and usually consists of four different polypeptide proteins chains: aα(s1)- and α(s2)-caseins, β-casein, and κ-casein (Walstra and Jenness, 1984), which have outstanding amphiphilic properties (Luo et al., 2014). CAS can endow food with certain functionalities, such as water solubility, emulsification, foamability and encapsulation ability. This is really useful because dairy products are considered to be good carriers of biologically active ingredients as they are an integral part of many people's diets. Additionally, CAS can adsorb at O/W interfaces and have ability to fast reduce interfacial tension during emulsification process. Eventually, a densely packed interface can be formed which may exhibit viscoelastic behavior. The characteristics of the interfaces are essential for understanding the stability of O/W emulsion systems. To better understanding the interaction mechanism between protein and nature aldehydes, the first objective the first objective is to investigate the effect of aldehydes on the interfacial and oscillatory dilatational properties of CAS stabilized droplet.

Moreover, fluorescence quenching was used to explore the binding properties among selected aldehydes and CAS. The effects of temperature and different concentration of aldehydes on CAS were carried out. In short, understanding the binding properties between nature aldehydes and dairy proteins will contribute food industries to formulate dairy-based products with more health benefit and functional properties.

2. Material and methods

2.1. Materials

Trans-cinnamaldehyde (TCA, 99%) and citral (99%) were purchased from Sigma-Aldrich (St Quentin Fallavier, France). Sodium caseinate (CAS) was purchased from Fisher Scientific (United Kingdom) and its protein content measured by the Kjeldahl method was 93.20% (nitrogen conversion factor N = 6.38). A medium chain triacylglycerol oil (MCT) was purchased from Gattefossé (Saint-Priest, France). Analytical grade imidazole ($C_3H_4N_2$), pure ethanol acetic acid, sodium hydroxide (NaOH), and hydrochloric acid (HCl), were purchased from Sigma-Aldrich Chimie (St Quentin Fallavier, France). All the solutions were prepared in deionized water.

2.2. Interfacial properties

2.2.1. Sample preparation

The aqueous phase for interfacial measurements was prepared by dispersing CAS powder (0.01 wt.%) into 100 mL of buffer solution (5 mmol/L acetic acid-imidazole, 0.05 wt.% sodium benzoate, pH 7). The protein solution was stirred at room temperature until it was completely dissolved. Oily phases were prepared by mixing TCA or citral (5 wt.%) with MCT under stirring until they are completely homogeneous. Pure MCT was used as control.

2.2.2. Droplet tension measurement

The O/W interfacial properties were measured by a Tracker automatic droplet tensiometer equipped with an oscillating drop accessor (Civrieux d'Azergue, France) at room temperature. The droplet profile was recorded every 0.02s by a connected digital camera. The values of interfacial tension were calculated by the Laplace equation (Castellani et al., 2010). According to the density of the oil phase, the rising drop method were chosen. Three different oil compositions (MCT, TCA/MCT, Citral/MCT). An initial droplet with a volume of 10 μL and a surface area of ~20 mm^2 was generated at the vertical needle, which was connected to an automatic syringe. The specific

low absorbance glass cuvette (8 ml) was filled with the aqueous phase contained 0.01 wt.% CAS. Interfacial tension was performed over a period of 10,800 s to monitor the protein adsorption kinetics. The oscillatory dilatational measurements (five cycles) were carried out at 10% amplitude and at a frequency of 0.1 Hz, which was tested to be within the linear viscoelastic regime. Further dilatational analysis was carried out during the protein adsorption phase, every 100 s.

2.3. Binding properties

2.3.1. Sample preparation

The CAS stock solution (0.048 wt.%, 20 μmol/L) was prepared by dispersing CAS powder into 100 mL of pH 7 acetic acid-imidazole buffer solution. The protein solution was stirred at room temperature until it was completely dissolved. The stock solution (160 μmol/L) of TCA and citral were prepared by dissolving 2 μL and 2.8 μL, respectively, into 100 mL of 10% ethanol pH 7 buffers. Stirring was continued until all of aldehydes were dissolved. Samples for ultraviolet fluorescence quenching test were prepared by mixed required volume of the stock solution of CAS (20 μmol/L), aldehydes and pH 7 buffer to the final volume of 4 mL. Therefore, each sample for fluorescence experiments has the fixed concentration (10 μmol/L) of CAS and various concentrations of TCA or citral (0, 5, 10, 20, 30, 40, 50, 60 and 80 μmol/L). Meanwhile, the highest resulting concentration of ethanol in each sample was 5 wt.% and it have been as control which does not affect the fluorescence intensity of the protein.

2.3.2. Ultraviolet (UV) Spectroscopy

To study the interaction of both aldehydes and CAS, changes in absorption of CAS in the absence and presence of various concentrations of two aldehydes was determined by an UV spectrophotometer (Jenway 3705, Villepinte, France) at room temperature and the wavelength range of 230 - 350 nm. Before each measurement, quartz cuvettes (1 cm path length) were filled with different samples in the dark for 30 min. Sample blank was buffer only.

2.3.3 Intrinsic fluorescence

Intrinsic fluorescence intensity of CAS was carried out in the absence and in the presence of various concentration of TCA or citral at room temperature by multimode microplate reader equipped with a temperature-controlled 96-wells microplate (Thermo Scientific™ Varioskan). The excitation wavelength was set at 280 nm and the emission spectrum was recorded in the

wavelength range of 298-550 nm with excitation and emission slit width each of 5 nm. Different samples were placed in the wells as the order of increasing the concentration of aldehydes molar ratio range from 0 to 80 μmol/L. The measurements were performed at 25, 30, 35, 40 °C, separately. Before each measurement, the mixture of CAS and aldehydes was incubated at room temperature in the dark for 30 minutes. The fluorescence intensity of acetate-imidazole buffer was used as a control.

2.4. Statistical analysis

All measurements were performed at least in triplicate. The results were then reported as averages and standard deviations of these measurements. Statistical analysis was performed by one-way ANOVA using SPSS software (IBM, version 19.0, USA).

3. Results and discussion

3.1. Impact of aldehydes on the interfacial behavior

The shape tensiometer has been used for the characterization of complex interfaces since it can provide dynamic information at the O/W interface. In the formation of O/W, hydrophobic groups in CAS will gradually adsorb to the surface of the oil droplets and then after subsequent rearrangements, become an interfacial layer. Fig. 1A showed the plot of interfacial tension as a function of time (t < 10,800 s) during the protein adsorption time in the different oily composition. In all three cases, the values of interfacial tension decreased with the time, at least during the initial adsorption period, which is related to different stages of protein adsorption (from protein diffusion to protein penetration, unfolding and rearrangement) (Felix et al., 2017). Pure MCT shows that the equilibrium interfacial tension was relatively high, about 13.56 mN/m, and when mixed with 5 wt.% TCA or citral, the equilibrium interfacial tension was significantly reduced to 9.12 and 11.27 mN/m, respectively. A similar result was observed by the study of cinnamaldehyde and whey protein (Felix et al., 2019). one possibility is that these two aldehydes are able to interact with proteins, leading to the additional rearrangements of CAS in the O/W interfaces, thereby resulting in a more densely packed structure, with lower interfacial tension (Dickinson, 1999). Interestingly, the image of oil droplets during measurement was recorded in 0, 3 and 15 h as shown in Fig. 1B. After 3 or 15 hours of protein adsorption, the pictures of oil droplet containing TCA showed obvious more turbid than others. This phenomenon can further support the possibility which TCA may have chemically reacted with the adsorbed CAS due to the presence of an aldehyde group in TCA molecules, thereby changing the structure and adsorbed CAS.

The change in interfacial tension with absorption time can be fitted with by the equation of Ward and Tordai equation (1) with slightly modification (Ward and Tordai, 1946).

$$\pi = 2C_0K_BT\left(\frac{Dt}{3.14}\right)^{1/2} \quad (1)$$

Where C_0 is the concentration of continuous phase, K_B is the Boltzmann constant, T is the absolute temperature, and D is the diffusion coefficient. The initial process of adsorption was assumed to be mainly controlled by the protein diffusion (Xiong et al., 2018). The plot of interfacial tension as function of $t^{1/2}$ is linear, and the diffusion rate (K_{diff}) can be calculated by the slope of this plot as

shown in Table 1. The highest K_{diff} rate was observed in the TCA/MCT oil phase, while there no obvious different observed in other two oily phases at the same CAS solution. These results suggested that for CAS stabilized interfaces, introducing citral into oily phase has only a marginal effect on protein diffusion. In addition, a small amount of TCA into oil phase can significantly improve the dispersibility and diffusion properties of CAS at the O/W interfaces. Several studies have indicated that TCA have the ability to interact with proteins, resulting in the formation of larger protein species and additional rearrangements in the O/W interface (Chen et al., 2018, 2017). After the initial diffusion stage, the adsorption kinetics become visibly slow which was caused by the energy barrier during the adsorption and rearrangement (Graham and Phillips, 1979). Moreover, the rate of penetration and rearrangement of adsorbed proteins at O/W interfaces can be analyzed by the first-order equation with slightly modification (Perez et al., 2009; Suttiprasit et al., 1992):

$$\ln\left[\frac{\pi_t-\pi_f}{\pi_0-\pi_f}\right] = -K_i t \quad (2)$$

Where π_0, π_f and π_t are the interfacial tension at the initial, final, and at any time, respectively, t is adsorption time and K_i is the first-order rate constant. Fig. 2 displayed a typical fitting curve of $\ln[(\pi_f-\pi_t)/(\pi_f-\pi_0)]$ as a function of the time. All of these curves include in two linear region which represent the first-order rate constant of penetration (K_p) and molecular reorganization (K_r) at the O/W interface, respectively. As shown in Table 1, the relative highest K_p value was found in the pure MCT and TCA/MCT oily phases, which suggested that TCA only have ability to promote the adsorption speed at the initial processing of protein absorption. Similar K_p values (Table 1) were found in pure MCT and TCA/MCT oil phase, which indicates that TCA does not have the ability to promote protein adsorption during the protein penetration process at O/W interface. This was probably attributed that TCA interact with adsorbed CAS molecular entanglement by forming a network structure, and then hindered the protein penetration at the interfacial layer. However, a relatively low K_p value was found in Citral/MCT oil and the lower R-value was obtained by a linear fit. This result may cause by the low density of citral (0.888 g/L). The low density of the mixed oily phase gradually changed the shape of droplets during the protein adsorption. On the other hand, the highest K_r value was found in the pure MCT oil phase, which be interpreted the fact that TCA and Citral were introduced into the oily phase and then decrease the polarity of the

oily phase (Liao et al., 2021), and lower hydrophobicity of oil phases will reduce the ability to attract emulsifiers.

3.2. Dilatational viscoelastic properties

Measuring the viscoelastic properties of the layers adsorbed at the O/W interface is an effective ways to evaluate the performance of the performance of the emulsion system (Chen et al., 2019). The dilatational elastic dilatational modulus were calculated by the first harmonic of the Fourier transform of the oscillating interfacial tension signal (Bagley and Torvik, 1983). Fig. 3 displayed the elastic module of oil-water interface with three different oily phases. After adsorption for 3 hours, the dilatational elastic modulus of all samples was significantly greater than the viscosity modulus (data not shown), indicating that the interface absorbed layer mainly exhibited the elastic behavior. In all cases, the value of elastic module gradually increased as a function of time due to the protein adsorption and the interaction between protein and protein. At the initial process of protein adsorption, the growth of elastic module was obvious and rapid and then it became gradually flattened. This tendency has been previously reported by other proteins, such as soy protein (Wang et al., 2020), bovine serum albumin (Tang and Shen, 2015), and pea protein (Sha et al., 2021). Interesting, the results confirmed that the addition of both aldehydes, especially TCA, can increase the elastic modules and result in a stronger protein network. These findings suggested that the interaction between protein and aldehydes had a vital influence on the protein adsorption at the O/W interface.

3.3. Ultraviolet Spectroscopy

UV spectroscopy is one of the generally used techniques for the illumination of the binding mode of small molecules to proteins, by measuring the changes in absorption and shift in the wavelength (Alam et al., 2018). The effect of various TCA and Citral concentrations (0 -80 μmol/L) on the CAS solution (10 μmol/L) was shown in Fig. 4. Pure TCA and Citral (40 μmol/L of, buffer) were used as the control. Fig. 4A showed that the mixture of CAS and TCA exhibited a maximum absorbance in the range of 280-290 nm and a distinct red shift was observed. Meanwhile, the intensity of the maximum absorbance was significantly improved with the increasing TCA concentration, indicating that there was interaction between TCA and CAS. Moreover, the adsorption peak at 280 nm of the mixture suggested that high concentrated TCA may cause the tryptophan, tyrosine and phenylalanine residues become more accessible and

therefore causes conformational changes in the protein (Sudha et al., 2016). As shown in Fig. 4B, pure citral exhibited a maximum absorbance around 245 nm and the mixture of CAS and TCA exhibited a similar maximum intensity around 280 nm, which suggesting there is no obvious interaction between CAS and citral.

3.4. Fluorescence spectra

The fluorescence spectra of CAS with the various concentrations of TCA and Citral at 25 ℃ are shown in Fig. 5. The CAS solution with the presence and absence of aldehydes possessed different fluorescence intensities which indicated the changes of environmental conditions. As several studies reported (Acharya et al., 2013), pure CAS solution exhibited an obvious emission band around 350 nm when the extraction band was 280 nm. After mixing with TCA (Fig. 5A), the fluorescence intensity of the maximum emission band decreased, which further indicated the occurrence of fluorescence quenching and the formation of complexes by TCA binding to aromatic residues of CAS. This fluorescence quenching have been supported by many previous studies (Mohammadian et al., 2019; Shi et al., 2015; Wu et al., 2021). With the subsequent increase in the TCA concentration, the maximum intensity further decreases with a gradual red shift, which may cause by the presence of binding sites near the fluorophores in the protein (Soltanabadi et al., 2018). However, as shown in Fig. 5B, the fluorescence intensity of CAS and citral only shows a very weak quenching phenomenon, which suggested CAS molecular could not provide a suitable environmental structure to bind citral molecular.

The quenching of CAS induced by TCA can be further analyzed by the Stern-Volmer equation (3), which can be dynamic, a collision between the fluorophore and quencher, or static, the formation of a ground-state complex between the fluorophore and quencher (Lakowicz, 2013).

$$\frac{F_0}{F} = 1 + k_q \tau_0 [Q] = 1 + K_{SV} \quad (3)$$

Where F_0 and F are the fluorescence intensities at 280 nm excitation wavelength before and after mixing with the quencher, respectively; k_q is the bimolecular quenching constant, τ_0 is the average lifetime of the fluorophore in the absence of quencher; [Q] is the concentration of the quencher, and K_{sv} is the Stern-Volmer quenching constant which can be calculated by linear regression of a plot of F_0/F against [Q]. The curve of F_0/F as a function of quencher concentration [Q] at different temperatures was shown as Fig. 6A. It is worth to note that, at high TCA concentration, an upward

deviation from linearity can be observed, which suggested that both dynamic and static quenching may occur in the fluorescence quenching mechanism. However, this equation is still not enough to distinguish the dynamic quenching form static (Acharya et al., 2013). An effective way to distinguish between dynamic quenching and static quenching can be to observe their bonding performance at different temperatures. The temperature increase can increase the quencher diffusion constant, which is usually accompanied by an increase in collisional quenching. For static quenching, the temperature have different effects (Acharya et al., 2013). Typically, this process will result in a decrease in the binding constant of the fluorophore quencher, and if the complexation reaction is exothermic, it will result in a decrease in the quenching of the static quencher. The modified Stern-Volmer equation (4) (Lakowicz and Weber, 1973) can be used to analysis when both static and dynamic quenching occur.

$$\frac{F_0}{F_0-F} = \frac{1}{f} + \frac{1}{f}\frac{1}{K_{SV}}\frac{1}{[Q]} \quad (4)$$

Where f is the available binding sites. When f is 1, the equation become the simple quenching process equation (3). The curve of $F_0/(F_0-F)$ as a function of quencher concentration $[Q]^{-1}$ at different temperatures was shown as Fig. 6B. At 25 °C, the quenching of CAS by TCA, K_{sv} is 2.25 × 10^{-4} M^{-1}. The fraction of the binding sites available for complexation was 1.63 higher than 1.0, which was probably attributed the occurrence of both dynamic and static quenching simultaneously. In addition, more binding sites could also be related with CAS which are a mixture of different casein protein, such as αs_1, αs_2, β and κ- casein and there caseins differ in the number of tryptophan residues and their location in the hydrophobic regions (Fu et al., 2014; Yazdi and Corredig, 2012).

The fluorescence lifetime of tryptophan has been reported around 3 ns (Lakowicz and Weber, 1973). The K_q, calculated by the equation (3), is 7.5 ×10^{12} M^{-1} per second at 25 °C, which is highly greater than the maximum dynamic quenching constant (~10×10^{10} $M^{-1}s^{-1}$). This indicated that there was a specific complex formation between CAS and TCA. For further analysis of quenching interaction, the binding constant and binding sites can be calculated by following modified Stern-Volmer equation (5).

$$\log\left[\frac{F_0-F}{F}\right] = \log K + n\log[Q] \quad (5)$$

Fig. 6C exhibited the curves of log $[(F_0-F)/F]$ against log [TCA] for the quenching of CAS

intrinsic fluorescence by TCA. Table 2 displayed the quenching parameter *K* (binding constant) and *n* (binding sites) at different temperatures. The large values of *K* were obtained at 25 and 30 °C which indicated the binding of TCA with CAS is highly favorable. As increasing temperatures, the binding constants gradually decreased which suggested that the complexation becomes weak at higher temperatures. Similar results was also found in the study of resveratrol and whey proteins by fluorescence spectroscopy (Hemar et al., 2011). The *n* values for binding of CAS and TCA were close to 1.0 for different temperatures.

To a better understanding of the thermodynamic of the interaction between CAS and TCA, Van't Hoff equation (6) was followed to calculate the change of enthalpy ΔH and entropy ΔS.

$$lnK = -\frac{\Delta H}{RT} + \frac{\Delta S}{R} \quad (6)$$

Where *K* is binding constant, *R* is the gas constant (8.314 J $mol^{-1}k^{-1}$) and *T* is the absolute temperature (K). Thereby, thermodynamic parameters ΔH and ΔS can be calculated by the slope and intercept of the curve of ln*K* as a function of 1/T. Fig. 7 showed the current Vant's Hoff fitting curve and it gives ΔH = −55.76 kJ mol^{-1}, ΔS= -86.05 J mol^{-1}. The free energy change (ΔG) can be then calculated from the equation (7) as follow:

$$\Delta G = \Delta H - T\Delta S \quad (7)$$

Table 2 summarized the thermodynamic parameters of binding between CAS and TCA. ΔG values at different temperatures are all negative, indicating the binding process of TCA and CAS is spontaneous and exothermic. The negative ΔH and ΔS values suggested that binding would be mainly driven by hydrogen bonds, which would promote a more ordered configuration of the solvent molecules around the complexes. This similar interaction was also found for other protein–small molecular combinations, such as zein proteins–resveratrol (Joye et al., 2015), crosslinked caseinate- quercetin, caseinate- kaempferol (Y.-J. Zhang et al., 2021) and bovine serum albumin- theaflavin-3,3′-digallate (Yu et al., 2022). Moreover, the high absolute value of ΔH even indicates that a covalent bond may be formed between CAS and TCA. Other complementary technologies are needed in the future to fully explore the exact type and strength of interaction between CAS and TCA. Nevertheless, the present work showed that TCA, a common flavoring in food, may be used as an interesting ingredient to improve the surface rheological properties of protein-based interfaces.

4. **Conclusion**

The interaction between aldehydes and CAS was investigated in the current study. Both aldehydes, especially TCA, have pronounced abilities to decrease the interfacial tension at O/W interface during adsorption process. Small amount of TCA introduced into oil phase can significantly improve the dispersibility and diffusion properties of CAS at the O/W interfaces. The results of dilatational measurements indicated the use of TCA into oily phase resulted in the development of stronger and more elastic interfaces. Furthermore, the fluorescence quenching test proved that TCA have more obvious quenching effect on CAS than citral. The large binding constants (1.78×10^5 M^{-1}) was calculated by Stern-Volmer equation which suggest that TCA has strong affinity with CAS. The negative free energy change for the binding between TCA and CAS indicated that complexation process is spontaneous. The negative enthalpy and negative entropy change suggested that the binding is mainly driven by formation of hydrogen. Entropy is unfavorable suggesting there is a loss of conformational freedom associated with binding. In summary, these nature aldehydes, could be a useful ingredient to improve the functionality of food protein-based products.

ACKNOWLEDGEMENTS

Wei Liao greatly thanks Chinese Scholarship Council for support.

CONFLICTS OF INTEREST

The author declares that there is no conflict of interest that could be perceived as prejudicing the impartiality of the research reported

References

Acharya, D.P., Sanguansri, L., Augustin, M.A., 2013. Binding of resveratrol with sodium caseinate in aqueous solutions. Food Chemistry 141, 1050-1054. https://doi.org/10.1016/j.foodchem.2013.03.037

Alam, Md.F., Varshney, S., Khan, M.A., Laskar, A.A., Younus, H., 2018. In vitro DNA binding studies of therapeutic and prophylactic drug citral. International Journal of Biological Macromolecules 113, 300-308. https://doi.org/10.1016/j.ijbiomac.2018.02.098

Asghari, G., Atri, M.S., Saboury, A.A., Mohadjerani, M., 2017. Study of the Interaction of Cinnamaldehyde with Alpha-lactalbumin: Spectroscopic and Molecular Docking Investigation. Biomacromolecular Journal 3, 123-132.

Azeredo, H.M., Waldron, K.W., 2016. Crosslinking in polysaccharide and protein films and coatings for food contact-A review. Trends in Food Science & Technology 52, 109-122.

Bagley, R.L., Torvik, P.J., 1983. A theoretical basis for the application of fractional calculus to viscoelasticity. Journal of Rheology 27, 201-210.

Banerjee, G., Chattopadhyay, P., 2019. Vanillin biotechnology: the perspectives and future. Journal of the Science of Food and Agriculture 99, 499-506.

Boeve, J., Joye, I.J., 2020. Food-grade strategies to increase stability of whey protein particles: Particle hardening through aldehyde treatment. Food Hydrocolloids 100, 105353. https://doi.org/10.1016/j.foodhyd.2019.105353

Castellani, O., Al-Assaf, S., Axelos, M., Phillips, G.O., Anton, M., 2010. Hydrocolloids with emulsifying capacity. Part 2-Adsorption properties at the n-hexadecane-Water interface. Food hydrocolloids 24, 121-130.

Chen, E., Cao, L., McClements, D.J., Liu, S., Li, B., Li, Y., 2018. Enhancement of physicochemical properties of whey protein-stabilized nanoemulsions by interfacial cross-linking using cinnamaldehyde. Food Hydrocolloids 77, 976-985. https://doi.org/10.1016/j.foodhyd.2017.11.047

Chen, E., Wu, S., McClements, D.J., Li, B., Li, Y., 2017. Influence of pH and cinnamaldehyde on the physical stability and lipolysis of whey protein isolate-stabilized emulsions. Food Hydrocolloids 69, 103-110. https://doi.org/10.1016/j.foodhyd.2017.01.028

Chen, W., Liang, G., Li, X., He, Z., Zeng, M., Gao, D., Qin, F., Goff, H.D., Chen, J., 2019. Impact of soy proteins, hydrolysates and monoglycerides at the oil/water interface in emulsions on interfacial properties and emulsion stability. Colloids and Surfaces B: Biointerfaces 177, 550-558.

Dickinson, E., 1999. Adsorbed protein layers at fluid interfaces: interactions, structure and surface rheology. Colloids and surfaces B: Biointerfaces 15, 161-176.

Dickinson, E., 1989. Protein adsorption at liquid interfaces and the relationship to foam stability, in: Foams: Physics, Chemistry and Structure. Springer, pp. 39-53.

Felix, M., Romero, A., Guerrero, A., 2017. Viscoelastic properties, microstructure and stability of high-oleic O/W emulsions stabilised by crayfish protein concentrate and xanthan gum. Food Hydrocolloids 64, 9-17.

Felix, M., Yang, J., Guerrero, A., Sagis, L.M.C., 2019. Effect of cinnamaldehyde on interfacial rheological properties of proteins adsorbed at O/W interfaces. Food Hydrocolloids 97, 105235. https://doi.org/10.1016/j.foodhyd.2019.105235

Fischer, P., Windhab, E.J., 2011. Rheology of food materials. Current Opinion in Colloid &

411 Interface Science 16, 36-40.
412 Fu, S., Shen, Z., Ajlouni, S., Ng, K., Sanguansri, L., Augustin, M.A., 2014. Interactions of
413 buttermilk with curcuminoids. Food Chemistry 149, 47-53.
414 https://doi.org/10.1016/j.foodchem.2013.10.049
415 Fuller, G.G., Vermant, J., 2012. Complex fluid-fluid interfaces: rheology and structure. Annual
416 review of chemical and biomolecular engineering 3, 519-543.
417 Glusac, J., Fishman, A., 2021. Enzymatic and chemical modification of zein for food application.
418 Trends in Food Science & Technology 112, 507-517.
419 https://doi.org/10.1016/j.tifs.2021.04.024
420 Graham, D.E., Phillips, M.C., 1979. Proteins at liquid interfaces: III. Molecular structures of
421 adsorbed films. Journal of Colloid and Interface Science 70, 427-439.
422 Guo, J., He, Z., Wu, S., Zeng, M., Chen, J., 2020. Effects of concentration of flavor compounds
423 on interaction between soy protein isolate and flavor compounds. Food Hydrocolloids
424 100, 105388.
425 Habeeb, A., Hiramoto, R., 1968. Reaction of proteins with glutaraldehyde. Archives of
426 biochemistry and biophysics 126, 16-26.
427 Hemar, Y., Gerbeaud, M., Oliver, C.M., Augustin, M.A., 2011. Investigation into the interaction
428 between resveratrol and whey proteins using fluorescence spectroscopy. International
429 journal of food science & technology 46, 2137-2144.
430 Joye, I.J., Davidov-Pardo, G., Ludescher, R.D., McClements, D.J., 2015. Fluorescence
431 quenching study of resveratrol binding to zein and gliadin: Towards a more rational
432 approach to resveratrol encapsulation using water-insoluble proteins. Food Chemistry
433 185, 261-267. https://doi.org/10.1016/j.foodchem.2015.03.128
434 Lakowicz, J.R., 2013. Principles of fluorescence spectroscopy. Springer science & business
435 media.
436 Lakowicz, J.R., Weber, G., 1973. Quenching of protein fluorescence by oxygen. Detection of
437 structural fluctuations in proteins on the nanosecond time scale. Biochemistry 12,
438 4171-4179.
439 Liao, W., Gharsallaoui, A., Dumas, E., Ghnimi, S., Elaissari, A., 2021. Effect of carrier oil on the
440 properties of sodium caseinate stabilized O/W nanoemulsions containing
441 Trans-cinnamaldehyde. LWT 146, 111655. https://doi.org/10.1016/j.lwt.2021.111655
442 Luo, Y., Pan, K., Zhong, Q., 2014. Physical, chemical and biochemical properties of casein
443 hydrolyzed by three proteases: partial characterizations. Food chemistry 155, 146-154.
444 Mohammadian, M., Salami, M., Momen, S., Alavi, F., Emam-Djomeh, Z., Moosavi-Movahedi,
445 A.A., 2019. Enhancing the aqueous solubility of curcumin at acidic condition through
446 the complexation with whey protein nanofibrils. Food Hydrocolloids 87, 902-914.
447 Perez, A.A., Carrara, C.R., Sánchez, C.C., Santiago, L.G., Patino, J.M.R., 2009. Interfacial
448 dynamic properties of whey protein concentrate/polysaccharide mixtures at neutral pH.
449 Food Hydrocolloids 23, 1253-1262.
450 Ribeiro, E.F., Morell, P., Nicoletti, V.R., Quiles, A., Hernando, I., 2021. Protein- and
451 polysaccharide-based particles used for Pickering emulsion stabilisation. Food
452 Hydrocolloids 119, 106839. https://doi.org/10.1016/j.foodhyd.2021.106839
453 Sha, L., Koosis, A.O., Wang, Q., True, A.D., Xiong, Y.L., 2021. Interfacial dilatational and
454 emulsifying properties of ultrasound-treated pea protein. Food Chemistry 350, 129271.

https://doi.org/10.1016/j.foodchem.2021.129271
Shen, S., Zhang, T., Yuan, Y., Lin, S., Xu, J., Ye, H., 2015. Effects of cinnamaldehyde on Escherichia coli and Staphylococcus aureus membrane. Food Control 47, 196-202.
Shi, J.-H., Chen, J., Wang, J., Zhu, Y.-Y., Wang, Q., 2015. Binding interaction of sorafenib with bovine serum albumin: Spectroscopic methodologies and molecular docking. Spectrochimica Acta Part A: Molecular and Biomolecular Spectroscopy 149, 630-637.
Soltanabadi, O., Atri, M.S., Bagheri, M., 2018. Spectroscopic analysis, docking and molecular dynamics simulation of the interaction of cinnamaldehyde with human serum albumin. Journal of Inclusion Phenomena and Macrocyclic Chemistry 91, 189-197.
Sudha, A., Srinivasan, P., Thamilarasan, V., Sengottuvelan, N., 2016. Exploring the binding mechanism of 5-hydroxy-3′, 4′, 7-trimethoxyflavone with bovine serum albumin: Spectroscopic and computational approach. Spectrochimica Acta Part A: Molecular and Biomolecular Spectroscopy 157, 170-181.
Suttiprasit, P., Krisdhasima, V., McGuire, J., 1992. The surface activity of α-lactalbumin, β-lactoglobulin, and bovine serum albumin: I. Surface tension measurements with single-component and mixed solutions. Journal of colloid and interface science 154, 316-326.
Tan, Y., Siebert, K.J., 2008. Modeling bovine serum albumin binding of flavor compounds (alcohols, aldehydes, esters, and ketones) as a function of molecular properties. Journal of food science 73, S56-S63.
Tang, C.-H., Shen, L., 2015. Dynamic adsorption and dilatational properties of BSA at oil/water interface: Role of conformational flexibility. Food Hydrocolloids 43, 388-399. https://doi.org/10.1016/j.foodhyd.2014.06.014
Tann, C.-M., Qi, D., Distefano, M.D., 2001. Enzyme design by chemical modification of protein scaffolds. Current Opinion in Chemical Biology 5, 696-704. https://doi.org/10.1016/S1367-5931(01)00268-X
Walstra, P., Jenness, R., 1984. Dairy chemistry & physics. John Wiley & Sons.
Wang, H., Zhu, J., Zhang, H., Chen, Q., Kong, B., 2021. Understanding interactions among aldehyde compounds and porcine myofibrillar proteins by spectroscopy and molecular dynamics simulations. Journal of Molecular Liquids 118190. https://doi.org/10.1016/j.molliq.2021.118190
Wang, K., Arntfield, S.D., 2015. Binding of selected volatile flavour mixture to salt-extracted canola and pea proteins and effect of heat treatment on flavour binding. Food Hydrocolloids 43, 410-417.
Wang, S., Yang, J., Shao, G., Qu, D., Zhao, H., Yang, L., Zhu, L., He, Y., Liu, H., Zhu, D., 2020. Soy protein isolated-soy hull polysaccharides stabilized O/W emulsion: Effect of polysaccharides concentration on the storage stability and interfacial rheological properties. Food Hydrocolloids 101, 105490. https://doi.org/10.1016/j.foodhyd.2019.105490
Ward, A.F.H., Tordai, L., 1946. Time-dependence of boundary tensions of solutions I. The role of diffusion in time-effects. The Journal of Chemical Physics 14, 453-461.
Weel, K.G., Boelrijk, A.E., Burger, J.J., Claassen, N.E., Gruppen, H., Voragen, A.G., Smit, G., 2003. Effect of whey protein on the in vivo release of aldehydes. Journal of agricultural and food chemistry 51, 4746-4752.

Weibel, H., Hansen, J., 1989. Interaction of cinnamaldehyde (a sensitizer in fragrance) with protein. Contact Dermatitis 20, 161-166.

Wu, C., Dong, H., Wang, P., Xu, X., Zhang, Y., Li, Y., 2021. Insight into the effect of charge regulation on the binding mechanism of curcumin to myofibrillar protein. Food Chemistry 352, 129395. https://doi.org/10.1016/j.foodchem.2021.129395

Xiong, W., Ren, C., Li, J., Li, B., 2018. Characterization and interfacial rheological properties of nanoparticles prepared by heat treatment of ovalbumin–carboxymethylcellulose complexes. Food Hydrocolloids 82, 355-362. https://doi.org/10.1016/j.foodhyd.2018.03.048

Yazdi, S.R., Corredig, M., 2012. Heating of milk alters the binding of curcumin to casein micelles. A fluorescence spectroscopy study. Food chemistry 132, 1143-1149.

Yu, X., Cai, X., Li, S., Luo, L., Wang, J., Wang, M., Zeng, L., 2022. Studies on the interactions of theaflavin-3,3′ -digallate with bovine serum albumin: Multi-spectroscopic analysis and molecular docking. Food Chemistry 366, 130422. https://doi.org/10.1016/j.foodchem.2021.130422

Zhang, X., Qi, B., Xie, F., Hu, M., Sun, Y., Han, L., Li, L., Zhang, S., Li, Y., 2021. Emulsion stability and dilatational rheological properties of soy/whey protein isolate complexes at the oil–water interface: Influence of pH. Food Hydrocolloids 113, 106391.

Zhang, Y.-J., Zhang, N., Zhao, X.-H., 2021. The non-covalent interaction between two polyphenols and caseinate as affected by two types of enzymatic protein crosslinking. Food Chemistry 364, 130375. https://doi.org/10.1016/j.foodchem.2021.130375

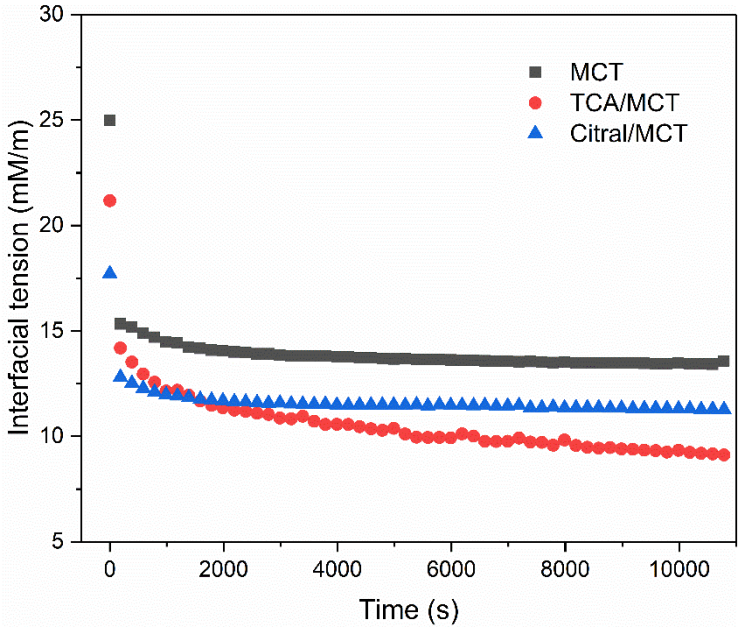

(A)

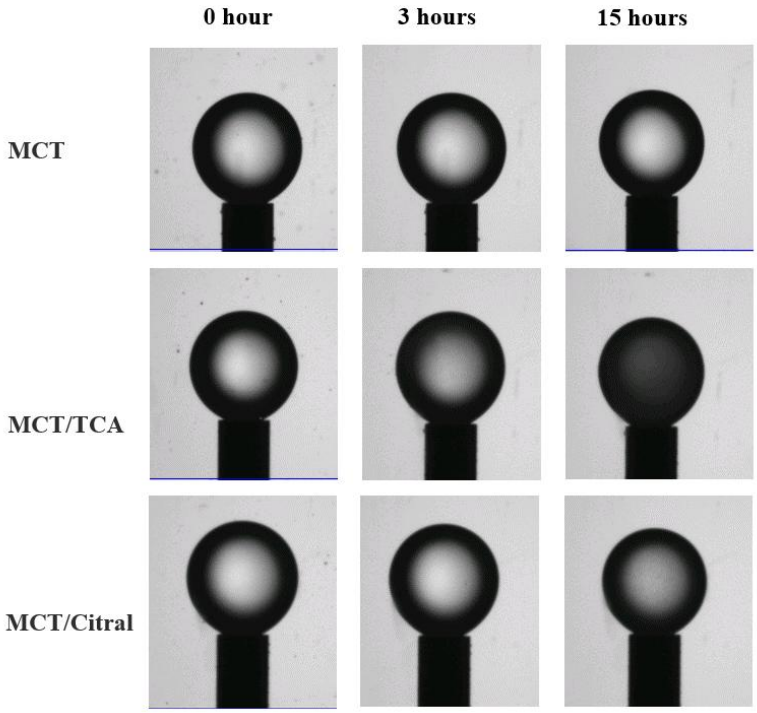

(B)

Fig. 1. (A) Interfacial tension over protein adsorption at O/W interface with or without TCA or Citral for 0.01% CAS solution at pH 7; (B) Visual image of oil droplets during measurement at different time.

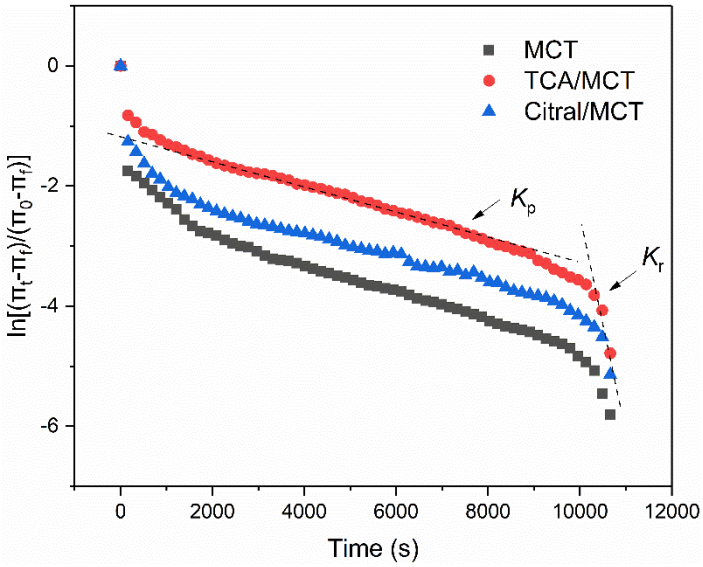

Fig. 2. The profile of the molecular penetration and configurational rearrangement steps over protein adsorption at the O/W interface with and without TCA or Citral for 0.01% CAS solution. *K*p and *K*r represents the first-order rate constants of penetration and rearrangement, respectively.

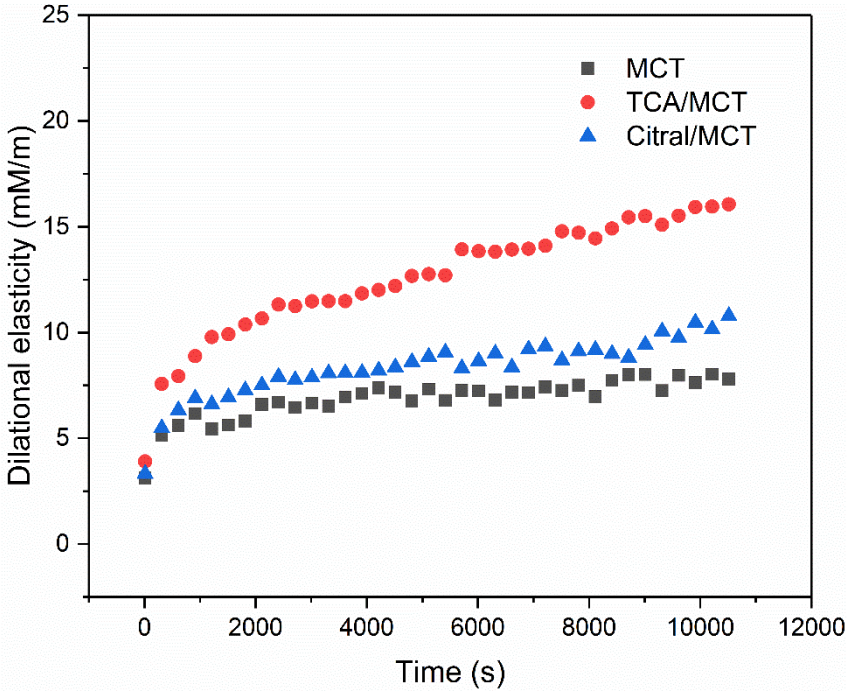

Fig. 3. Dilatational elasticity over protein adsorption at O/W interface with and without TCA or Citral for 0.01% CAS solution.

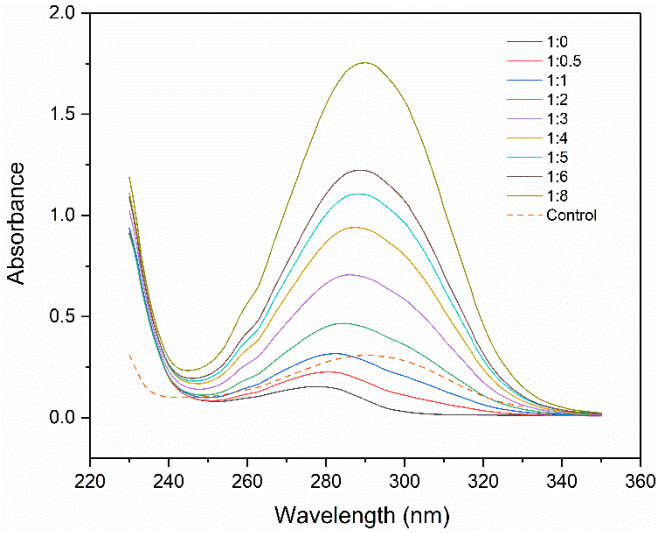

(A)

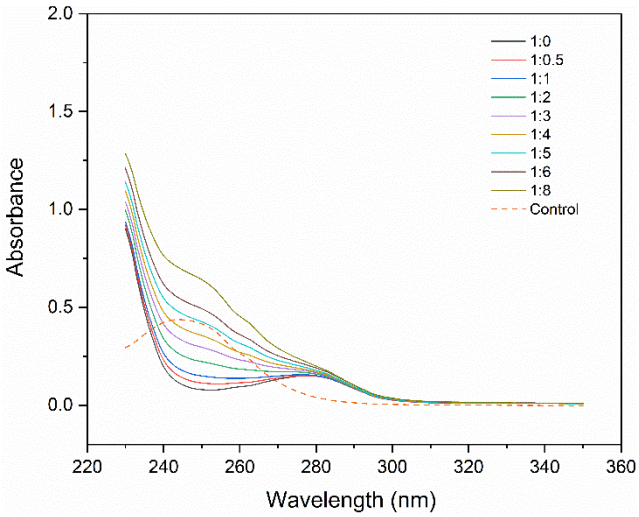

(B)

Fig. 4. Absorption spectra of 10 μmol/L CAS solution in the presence of increasing (A) TCA or (B) citral concentrations (0 - 80 μmol/L) at 25 °C.

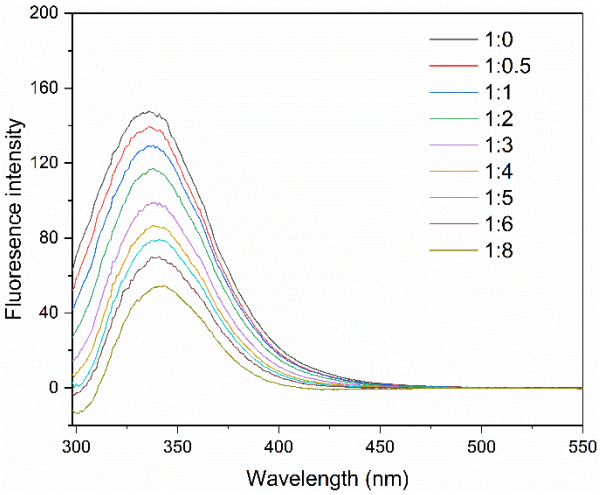

(A)

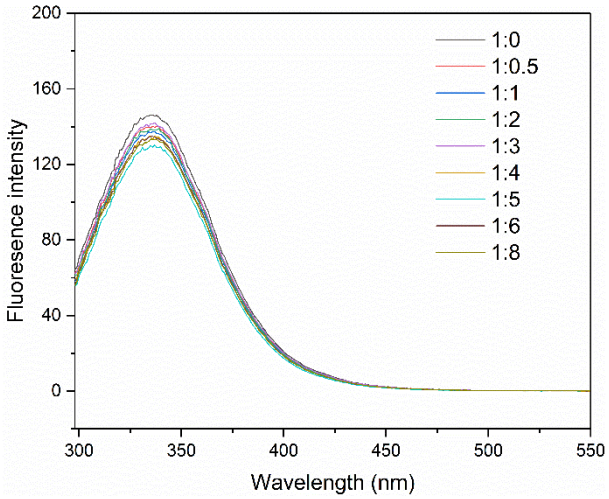

(B)

Fig. 5. Fluorescence spectra of 10 μmol/L CAS solution at the excitation wavelength of 280 nm in the presence of increasing (A) TCA or (B) citral concentrations (0 - 80 μmol/L) at 25 °C.

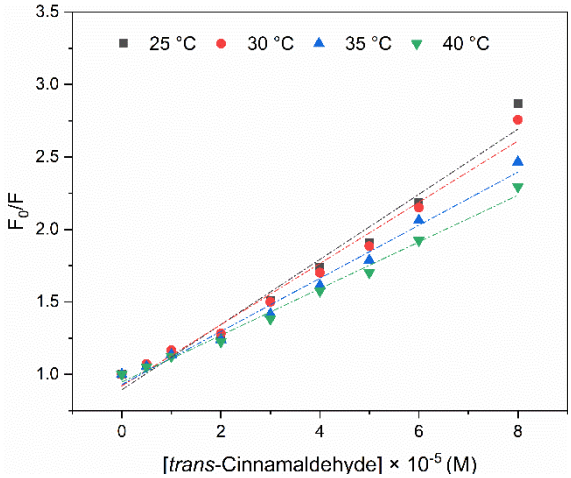

(A)

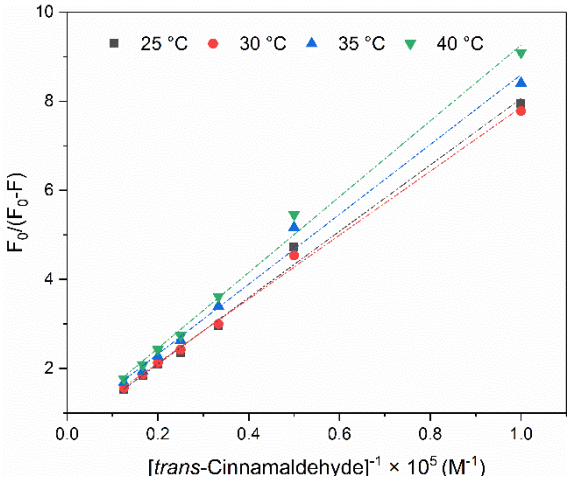

(B)

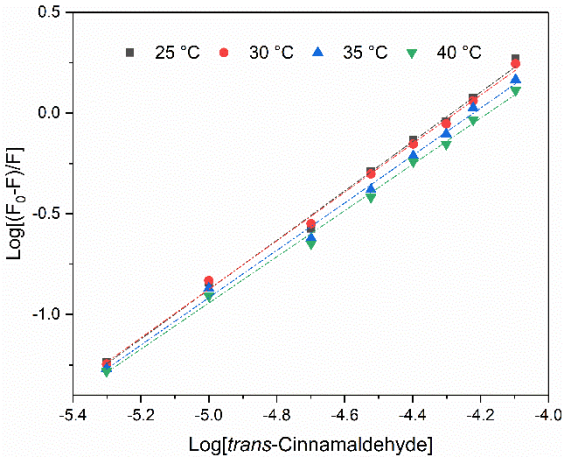

(C)

Fig. 6. (A) Stern–Volmer plot of F_0/F as a function of the concentration of TCA at different temperatures; (B) Plot of $(F_0/(F_0-F))$ as a function of the reciprocal of concentration of TCA at different temperatures; (C) Plot of Log $[(F_0 - F)/F]$ as a function of log of the concentration of TCA at different temperatures; F_0 and F represent the fluorescence intensity in the absence and

presence of TCA, respectively.

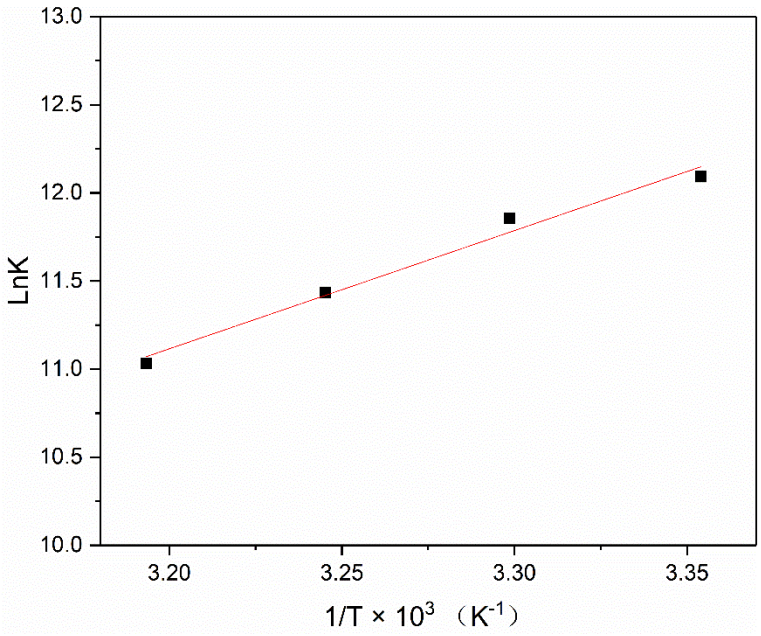

Fig. 7. The Van't Hoff plot of ln K as a function of 1/T (K) for the binding of TCA with CAS solution.

Table 1. the apparent diffusion rate (K_{diff}), constants of penetration and structural rearrangement at the interface (K_p and K_r), and interfacial pressure at the end of adsorption (π_{10800}) for different oily phase in 0.01% CAS solution.

Samples	K_{diff} (mN/m/s$^{1/2}$)	$K_p \times 10^4$	$K_r \times 10^4$	π_{10800} (mN/m)
MCT	-0.090 ± 0.016	-2.151 ± 0.005	-8.543 ± 0.005	13.56
TCA/MCT	-0.122 ± 0.006	-2.178 ± 0.001	-7.046 ± 0.009	9.12
Citral/MCT	-0.081 ± 0.010	-1.820 ± 0.002	-5.626 ± 0.002	11.27

Table 2. Variation of binding constant *K* and the number of binding site *n* as a function of temperature and thermodynamic parameters of binding calculated using Van't Hoff equation.

T (°C)	*K*	*n*	r^2	Δ*H* (kJ mol^{-1})	Δ*S* (J mol^{-1} K^{-1})	Δ*G* (kJ mol^{-1})
25	1.782×10^5	1.225	0.996	−55.76	-86.05	-30.1051
30	1.406×10^5	1.204	0.997			-29.6748
35	0.925×10^5	1.177	0.996			-29.2446
40	0.618×10^5	1.147	0.997			-28.8143